



# Finite Element Simulation of LCF Behaviour of SA 333 C-MN Steel.

A.BHOWMICK

P.G Student

Department of Mechanical Engineering  
 Jalpaiguri Government Engineering College  
 West Bengal, India

J.SHIT

Associate Professor

Department of Mechanical Engineering  
 Jalpaiguri Government Engineering College  
 West Bengal, India

**Abstract**—Finite Element simulation to characterize the LCF behavior of Sa 333 C-Mn Steel is studied in this paper. Experiment and Finite Element simulation are done together. LCF parameters of the material are calibrated and tuned from the experimental results. Non linear version of Ziegler kinematic hardening material model is used to address the stable hysteresis cycles of the material. Cyclic hardening phenomenon is addressed by introducing cyclic hardening in the material model. The elastic plastic FE code ABAQUS is used for finite element simulation of LCF behavior. The plastic modulus formulation with zeigler kinematic hardening rule and exponential isotropic hardening rule has been used for simulation. Using the incremental plasticity theories the cyclic plastic stress-strain responses were analyzed and the results obtained from FE simulations have been compared with the experimental results at different strain amplitudes. Variation of cyclic yield stress with strain amplitudes has also been studied in this paper.

**Keywords**- Cyclic hardening, elastic-plastic finite element, incremental plasticity, Kinematic hardening, LCF, plastic modulus.

## I. INTRODUCTION

The material Sa 333 C-Mn steel is used in Indian PHWR as primary heat transport (PHT) pipe material. The cyclic plastic behavior includes symmetric strain controlled low cycle fatigue, cyclic hardening/ softening character of the material in transition cycles (from virgin state to saturated state) and uniaxial ratcheting phenomenon for non-symmetric stress controlled cyclic loading. Low cycle fatigue [1-3] must be considered during design of nuclear pressure vessels, steam turbines and other type of power machineries where life is nominally characterized as a function of the strain range and the component fails after a small number of cycles at a high stress, and the deformation is largely plastic. Experimental observation shows that various cyclic plastic behavior [4-7] of the material. Those are i.) Bauschinger effect ii.) Cyclic hardening [8]. Above all, there is additional hardening due to non proportional loading path. This is generally modeled by using proper evolution laws of back stress tensor. A simplest choice is a linear kinematic hardening law proposed by Prager [9]. Armstrong and Frederick [10] introduced a nonlinear law with recall term. Armstrong – Frederick law is modified by Chaboche [11], Ohno [12] for better matching with experimental results. Cyclic hardening of this material is observed during strain controlled symmetric tension- compression cyclic loading. Hardening stress gets saturated after few cycles which depend on the material. Some materials exhibits cyclic softening during symmetric loading. During first few cycles the rate of hardening is relatively high and gradually drops down to a constant value. Chaboche [13], Ohno and

Wang [14], Jiang and Sehitoglu [15],Bari and Hassan [16], and many others researchers developed their cyclic plasticity models for improving cyclic plastic phenomena of the material. The aim of this present work is to characterize the cyclic plastic behavior of this material i.e the simulation of stable hysteresis loops for different strain amplitudes and simulation of cyclic hardening with no of cycles for various strain amplitudes. Another aim of this work is to study the variation of cyclic yield stress with the various strain amplitude.

## II. MATERIAL CHARACTERIZATION

### A. Low cycle fatigue tests

The material selected for investigation is Sa 333 Gr.6 Carbon Manganese steel used in primary heat transport pipes of Indian in PHWR. Uniaxial cyclic experiments are performed at room temperature on 8mm diameter fatigue specimens, gauge length 18mm made of Sa 333 Gr.6 Carbon Manganese steel(Fig-2.1) under strain controlled (Fig-2.2) mode. A 100 KN servo-hydraulic universal testing machine (Instron UTM) is used. A 12.5mm gauge length extensometer is attached to the specimen to measure the strain during the test. The extensometer is capable of measuring 20% strain. The strain-controlled tests are performed on the specimens for symmetric tension-compression strain cycles with the strain amplitudes  $\pm 0.50\%$ ,  $\pm 0.70\%$ ,  $\pm 0.85\%$ ,  $\pm 1.00\%$ ,  $\pm 1.20\%$ ,  $\pm 1.4\%$  and  $1.6\%$  for low cycle fatigue. During the test triangular wave form is used with a constant strain rate of 10-3/s. The frequency is adjusted accordingly. The stabilized hysteresis loops of  $\sigma-\epsilon_p$  for various strain amplitudes are obtained from the test (Fig-2.3). This plot is used to

calculate the kinematic hardening coefficients. The kinematic hardening coefficients obtained from the experiments are used in FE simulation. Cyclic hardening is observed in the experiment as shown in Fig-2.4 .The material gets saturated after 30 cycles and the stabilized loop is obtained for all the cases. The variation of cyclic yield stress with strain amplitudes is obtained in Fig-2.3. The cyclic yield stress  $\sigma_{yc}$  is calculated from the linear part of the

loading branch which is equal to  $2\sigma_{yc}$ . Those values are listed in Table-2.2.

**TABLE-2.2: VARIATION OF CYCLIC YIELD STRESS WITH STRAIN AMPLITUDES**

Strain amplitudes	$\sigma_{yc}$ (MPa)
0.85%	227.5
1.0%	237.5
1.2%	245
1.6%	260

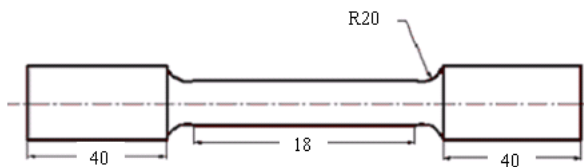


**Figure 2.1: Uniaxial Fatigue Specimen.**

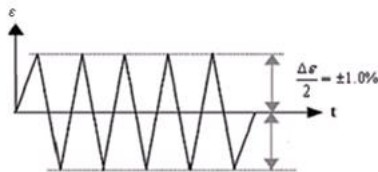


**Figure 2.2: Loading history during strain-controlled test.**

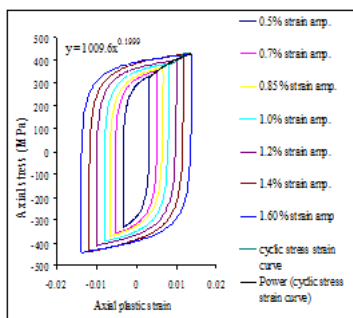


**Figure 2.3: Stabilized hysteresis plots for different strain amplitudes with cyclic stress-strain curve.**

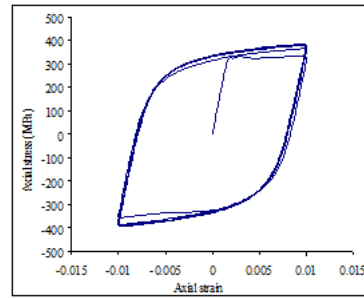


**Figure 2.4: Experimental stress strain response up to 30th cycles for 1% strain amplitude curve.**

### III. FINITE ELEMENT SIMULATION

#### 3.1 Modeling of cyclic plasticity:

The cyclic behavior of the material was modeled using Von mises yield function, flow rules and the nonlinear isotropic-kinematic hardening model and consistency condition as follows

##### 3.1.1 Yield Function: -

The Von mises yield function is as follows.

$$\Phi = \frac{3}{2}(S_{ij} - \alpha_{ij})(S_{ij} - \alpha_{ij}) - \sigma_c^2 = 0 \quad \dots(3.1)$$

$\sigma_c$  = Current flow stress of matrix material,

$S_{ij}$  = deviatoric part of stress tensor,

$$\sigma_{ij} = S_{ij} + \sigma_m \delta_{ij},$$

$\sigma_m$  = Mean Stress,

$\alpha_{ij}$  = back stress tensor, also deviatoric in nature.

##### 3.1.2 The Flow Rule:

The Plastic strain rate,  $\dot{\epsilon}_{ij}^p$ , follows from the flow rules as

$$\dot{\epsilon}_{ij}^p = \dot{\epsilon}^p \frac{\partial \Phi}{\partial \sigma_{ij}} \quad \dots(3.2)$$

Here,  $\dot{\epsilon}^p$  is a scalar multiplier or equivalent plastic strain rate.

Which yields

$$\dot{\epsilon}^p = \sqrt{\frac{2}{3} \dot{\epsilon}_{ij}^p \dot{\epsilon}_{ij}^p} = \lambda \left[ \frac{2}{3} \frac{\partial \phi}{\partial \sigma_{ij}} \frac{\partial \phi}{\partial \sigma_{ij}} \right]^{\frac{1}{2}}$$

### 3.1.3 Non linear version of Ziegler’s kinematic hardening law:

The kinematic hardening component is defined to be an additive combination of a purely kinematic term (linear Ziegler[17] hardening law) and a relaxation term (the recall term), which introduces the non linearity. When temperature and field variable dependencies are omitted, the hardening law is

$$\dot{\alpha} = C \frac{1}{\sigma_c} (\sigma - \alpha) \dot{\epsilon}^p - \gamma \alpha \dot{\epsilon}^p \quad \dots(3.3)$$

Where,  $C$  and  $\gamma$  are material parameters that is calibrated from cyclic test data.  $C$  is the initial kinematic hardening modulus, and  $\gamma$  determines the rate at which the kinematic hardening modulus decreases with increasing plastic deformation. The kinematic hardening law can be separated into a deviatoric part and a hydrostatic part; only the deviatoric part has an effect on the material behavior. When  $C$  and  $\gamma$  are zero, the model reduces to an isotropic hardening model. When  $\gamma$  is zero, the linear Ziegler hardening law is recovered. The isotropic hardening behavior of the model

defines the evolution of the yield surface size,  $\sigma_c$  as a function of the equivalent plastic strain  $\bar{\epsilon}^p$ . This evolution can be introduced by specifying  $\sigma_c$  directly as a function of  $\bar{\epsilon}^p$ .

For the isotropic hardening rule, Chaboche [18] proposed the following equation:

$$\dot{R}(\bar{\epsilon}^p) = b \left( Q_\infty - e^{-b \bar{\epsilon}^p} \right)$$

where  $Q_\infty$  and  $b$  are the isotropic hardening material parameters are computed from experimental stress–strain loop results of LCF test of plain fatigue specimens. Using the initial condition  $R(\bar{\epsilon}^p) = 0$ , on integration of the above differential equation, we get

$$R = Q_\infty \left( 1 - e^{-b \bar{\epsilon}^p} \right)$$

Now the simple exponential law is

$$\sigma^c = \sigma|_0 + Q_\infty \left( 1 - e^{-b \bar{\epsilon}^p} \right) \quad \dots(3.4)$$

Where,  $\sigma|_0$  is the yield stress at zero plastic strain and  $Q_\infty$  and  $b$  are material parameters.  $Q_\infty$  is the maximum change in the size of the yield surface, and ‘b’ defines the rate at which the size of

the yield surface changes as plastic straining develops. When the equivalent stress defining the size of the yield surface remains constant ( $\sigma_c = \sigma|_0$ ), the model reduces to a nonlinear kinematic hardening model.

### 3.1.4 Consistency condition:

During plastic deformation stress vector remain on the yield surface. This leads to consistency equation,  $\dot{\Phi} = 0$

Finally, the elastic–plastic tensor,  $D_{ijkl}$ , is represented as:

$$D_{ijkl} = E_{ijkl} - \frac{1}{H} E_{ijkl} \frac{\partial \phi}{\partial \sigma_{mn}} E_{klpq} \frac{\partial \phi}{\partial \sigma_{op}}$$

Calibration of kinematic hardening coefficient for Ziegler law for the material Sa 333 C-Mn steel.

To simulate the saturated loops at different strain amplitude the coefficients-  $C$  and  $\gamma$  of Ziegler kinematic hardening rule are calculated from stabilized hysteresis loop plot of  $\sigma$ - $\epsilon$ p. Saturated hysteresis loop for  $\pm 1.6\%$  strain amplitude is used for calculating the values of  $C$  and  $\gamma$ . Those are finally tuned to have a good match with the experimental results. Table 3.1 shows the values of Ziegler kinematic hardening coefficient  $C$  and  $\gamma$  along with other mechanical properties of Sa 333 C-Mn steel. Table 3.2 shows the cyclic hardening parameters as used in ABAQUS package.

**TABLE-3.1 KINEMATIC HARDENING COEFFICIENTS OF ZIEGLER’S NONLINEAR KINEMATIC HARDENING RULE FOR SA 333 C-MN STEEL.**

Young’s Modulus (E) (GPa)	Poisson’s Ratio	Yield Strength ( $\sigma_c$ ) (MPa)	C (MPa)	$\gamma$
200	0.3	275	3200 0	21 4

**TABLE-3.2 CYCLIC HARDENING PARAMETERS FOR SA 333 C-MN STEEL AS USED IN ABAQUS PACKAGE**

C (MPa)	$\gamma$	$Q_\infty$ (MPa)	b
32000	214	18.5	2.5

#### IV. SIMULATION OF STABLE HYSTERESIS LOOPS AND CYCLIC HARDENING FOR VARIOUS STRAIN AMPLITUDE

Strain controlled tension compression loading is implemented on a round bar specimen for simulation of stable hysteresis loops and cyclic hardening for various strain amplitude. The Ziegler isotropic-kinematic hardening laws have been used for simulation. The non-linear version of Ziegler kinematic hardening rule plugged in elasto-plastic finite element FE code ABAQUS. The working length of the specimen is discretized with eight noded axisymmetric element of mesh size as 0.2mmX 0.2mm. For symmetry in geometry, loading and boundary conditions one quarter of the specimen is discretized. Fig.8 shows FE mesh of the specimen together with boundary conditions. FE computations are done with Von Mises yield function(equation 3.1), flow rules and the kinematic hardening rules together with the consistency condition, as discussed earlier. The axial component of stress strain values, calculated at the center node of the specimen, is taken as the representative axial stress and axial strain values of the specimen. The cyclic loading is plastic strain controlled. A triangular waveform is used for symmetric cyclic load time history. The saturated values of Ziegler kinematic hardening coefficients as obtained from experimental saturated loop of 1.6% strain amplitudes are used to simulate the hysteresis loops and peak stress vs. cycles of all the strain amplitudes.

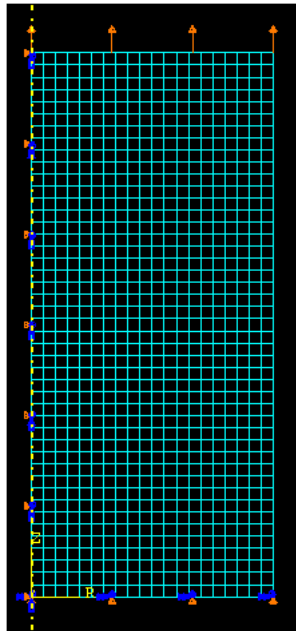


**Figure 4.1** FE mesh of the specimen with boundary condition.

Fig-4.2 (a,b,c,d) show the simulation results for stable hysteresis loop using Ziegler’s non-linear

model. Those results are compared with experimental stable hysteresis loops (at 30th cycle). Ziegler’s coefficients are obtained from experimental stable hysteresis loop for 1.6% strain amplitudes are used for other strain amplitudes also.

The cyclic yield stress  $\sigma_{yc}$  is taken as 275MPa for all strain amplitudes. For the strain amplitude  $\pm 1.6\%$ , the simulated results closely follow the experimental results in the non-linear portion of the loading/unloading branch. Still there is some mismatch at the elastic plastic knee region. It is expected that the prediction from the simulated results for  $\pm 1.6\%$  strain amplitudes will show better match with the experimental values because the Ziegler’s kinematic hardening coefficients are calibrated from  $\pm 1.6\%$  strain amplitude experimental values. For other strain amplitudes the mismatch in the non-linear part of loading/unloading branch is predominant.

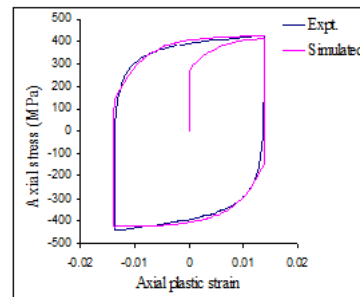


**Figure 4.2(a)** Strain amplitude  $\pm 1.6\%$ .

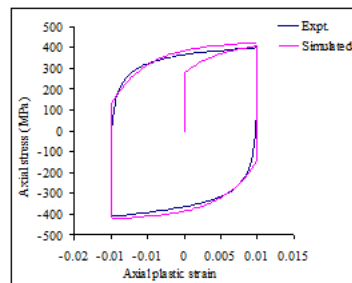


**Figure 4.2(b)** Strain amplitude  $\pm 1.2\%$ .

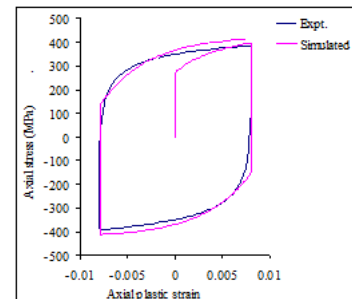


**Figure 4.2(c)** Strain amplitude  $\pm 1.0\%$

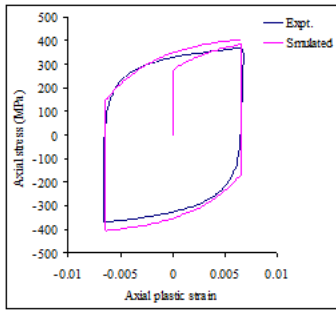


Figure 4.2 (d) Strain amplitude  $\pm 0.85\%$

Fig-4.2 (a,b,c,d): Stable stress strain hysteresis loop for various strain amplitudes using Ziegler rule (ABAQUS results)

( $\sigma_0 = 275 \text{ MPa}$ ) (Material Sa 333 C-Mn steel).

Now the size of the yield surface is chosen to be different for different strain amplitude. These are 260(MPa), 245(MPa), 237.5(MPa) and 227.5 (MPa) for  $\pm 1.6\%$ ,  $\pm 1.2\%$ ,  $\pm 1.0\%$  &  $\pm 0.85\%$  strain amplitudes respectively. It is found that the simulated hysteresis loops at saturation (after 30 cycles) match well with the experimental results for the material Sa 333 Carbon Manganese steel.

Fig 4.3 (a,b,c & d) show similar results for the simulation of stable hysteresis loops for different strain amplitudes as obtained by using the Ziegler model with isotropic hardening in ABAQUS FE package. Here also the saturated loops are obtained after cycling of 30 cycles.

Fig 4.4(a,b,c & d) represent the simulated peak stress vs cycles as obtained by using Ziegler kinematic hardening model together with isotropic hardening. It is seen that the matching is satisfactory in engineering sense.

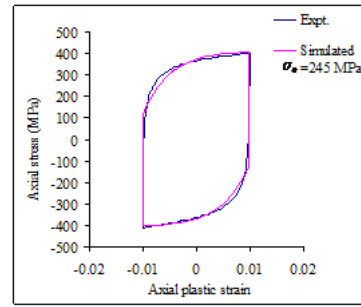


Figure 4.3 (b) Strain amplitude  $\pm 1.2\%$ .

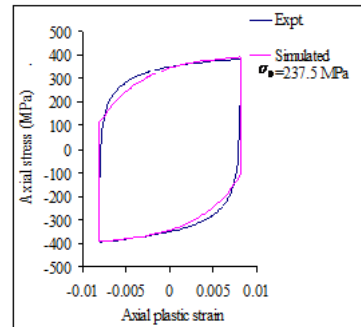


Figure 4.3(c) Strain amplitude  $\pm 1.0\%$ .

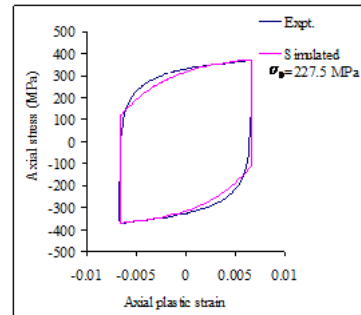


Figure 4.3 (d) Strain amplitude  $\pm 0.85\%$ .

Fig-4.3 (a, b, c & d): Saturated stress – strain hysteresis loop for different strain amplitudes using Ziegler rule with isotropic hardening (ABAQUS results).

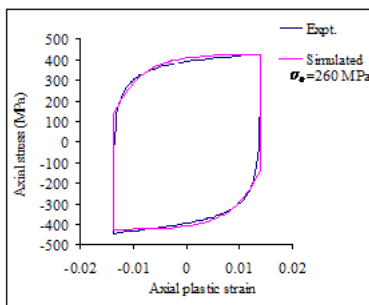


Figure 4.3(a) Strain amplitude  $\pm 1.6\%$ .

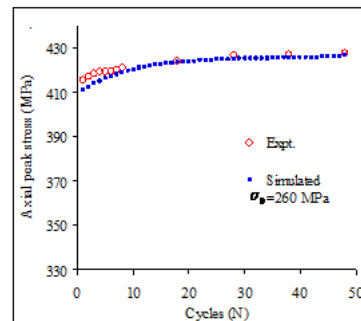


Figure 4.4 (a) Strain amplitude  $\pm 1.6\%$ .



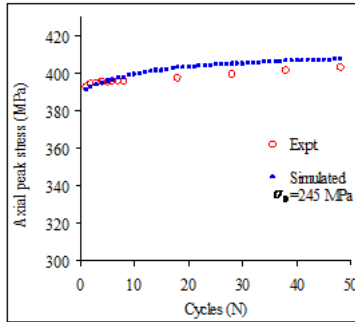


Figure 4.4 (b) Strain amplitude  $\pm 1.2\%$ .

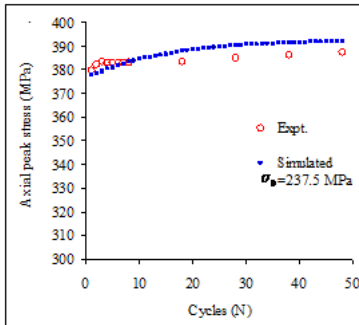


Figure 4.4 (c) Strain amplitude  $\pm 1.0\%$ .

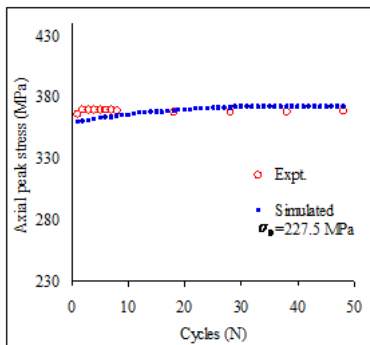


Figure 4.4 (d) Strain amplitude  $\pm 0.85\%$ .

Fig-4.4 (a, b, c & d): Variation of peak stress with no of cycles for different strain amplitudes using Ziegler KH rule with isotropic hardening (ABAQUS results).

## V. DISCUSSION & CONCLUSIONS

The present work is an attempt for verifying the cyclic yield stress that depends on strain amplitude and corresponding FE simulation of LCF behavior of SA 333 C-Mn steel. The size of the yield surface has been chosen as 260(MPa), 245(MPa), 237.5(MPa) and 227.5 (MPa) for  $\pm 1.6\%$ ,  $\pm 1.2\%$ ,  $\pm 1.0\%$  &  $\pm 0.85\%$  strain amplitudes respectively. The simulated hysteresis loops at saturation match well with the experimental results for  $\pm 1.6\%$ ,  $\pm 1.2\%$ ,  $\pm 1.0\%$  &  $\pm 0.85\%$  strain amplitudes respectively as shown in the above Figure. Comparison between simulated and experimental loop is satisfactory in engineering sense. But there is some mismatch at the elasticity

plastic knee region. This is because of using ziegler's single segmented non linear kinematic hardening law which has the same deficiency as the single segmented Armstrong Frederick law, however results can be improved by using Chaboche's 3 segmented non linear kinematic hardening model. The next attempt of this study is to simulate peak stress value with no. of cycles for various strains amplitudes with varying yield stress i.e . 260(MPa), 245(MPa), 237.5(MPa) and 227.5 (MPa) for  $\pm 1.6\%$ ,  $\pm 1.2\%$ ,  $\pm 1.0\%$  &  $\pm 0.85\%$  strain amplitudes respectively. It is seen that the matching is satisfactory in engineering sense.

## VI. REFERENCES

- [1]. Lim Jae-Yong, Hong Seong-Gu, Lee Soon-Bok. Application of local stress-strain approaches in the prediction of fatigue crack initiation life for cyclically non-stabilized and non-masing steel. International journal of fatigue 27 (2005) 1653-1660.
- [2]. Dutta A, Dhar S, Acharyya S.K. Material characterization of SS 316 in low cycle fatigue loading. J Mater Sci (2010) 45: 1782-1789.
- [3]. Shit J, Dhar S, Acharyya S. Modeling and Finite Element Simulation of Low Cycle Fatigue Behavior of 316 SS. 6th International Conference on Creep, Fatigue and Creep-Fatigue Interaction [CF-6]. Procedia Engineering 55 (2013) 774 – 779.
- [4]. Paul Surajit Kumar, Sivaprasad S, Dhar S, Tarafder M, Tarafdaer S. Simulation of cyclic plastic deformation response in SA 333 C-Mn steel by a kinematic hardening model. Computational material science 48 (2010) 662-671.
- [5]. Hassan Tasnim, Kyriakides Stelios. Ratcheting in Cyclic Plasticity, Part I: Uniaxial Behavior. International journal of plasticity, vol 8, pp. 91-116, 1992.
- [6]. Hassan Tasnim, Corona Edmundo, and Kyriakides Stelios. Ratcheting in Cyclic Plasticity, Part II: Multiaxial Behavior. International journal of plasticity, vol 8, pp.117-146, 1992.
- [7]. Shit J, Dhar S, Acharyya S. Experimental and numerical simulation of carbon and manganese steel for cyclic plastic behavior. International Journal of Engineering, Science Technology Vol. 2, No. 4, 2010, pp. 71-84.
- [8]. Kang Guozheng, Ohno Nobutada, Nebu Akira. Constitutive modeling of strain range dependent cyclic hardening. International journal of plasticity 19 (2003) 1801-1819.

- [9]. Prager. W 1956. A new method of analyzing stresses and strains in work hardening plastic solids. ASME J. Appl.Mech Vol. 23, pp. 493-496.
- [10]. Armstrong P.J, Frederick C.O. 1966. A mathematical representation of the multiaxial Bauschinger effect. CEGB; Report No RD/B/N731.
- [11]. Chaboche J.L. 1986. Time independent constitutive theories for cyclic plastic. Int. J.L.Plasticity, Vol. 2, No. 2, pp. 149-188.
- [12]. Ohno N. A , 1982. Constitutive model of cyclic plasticity with a non hardening strain region. ASME, J.L. Appl. Mech, Vol-49, pp.721-727.
- [13]. Chaboche, J.L., Dang-Van, K., Cordier, G., 1979. Modelization of the strain memory effect on the cyclic hardening of 316 stainless steel. Proc. of the 5th International Conference on SMiRT, Div. L, Berlin, Germany.
- [14]. Ohno, N., Wang, J.,D., 1993. Kinematic hardening rules with critical state of dynamic recovery, part I: formulations and basic features for ratcheting behavior. Int. J. Plasticity. 9, 375-390.
- [15]. Jiang, Y., Sehitoglu, H., 1996. Comments on the Mroz multiple surface type plasticity models. International Journal of Solids and Structures. 33, 1053-1068.
- [16]. Bari, M.S., 2001. Constitutive Modeling for Cyclic Plasticity and Ratcheting,, Ph.D.Dissertation, North Carolina State university.
- [17]. Ziegler, H. (1959). ‘A Modification of Prager's Hardening Rule’. Quarterly of Applied Mechanics, Vol 17, pp. 55-65.
- [18]. Chaboche JL, Nouailhas D (1989) Trans ASME 111:384

## VII. AUTHOR'S PROFILE



**Sri Avijit Bhowmick** is a Post Graduate student of Mechanical Engineering of Jalpaiguri Government Engineering College, West Bengal. He has completed his B.E in Mechanical Engineering from SIEM, West Bengal in 2013.



**Dr. Jagabandhu Shit** is an Associate Professor of Mechanical Engineering at Jalpaiguri Govt. Engg. College, West Bengal. He is engaged in teaching and research activities since the last 10 years. His field of specialization is Plasticity. He is doing his research work in the area of LCF and ratcheting. He has published several papers in various national, international conferences and journals. He has completed his PG from Mechanical Engineering Department Jadavpur University.